

**UNIVERSITY OF OXFORD**

**DEPARTMENT OF ENGINEERING SCIENCE**

**REPORT**



WIND TUNNEL PRESSURE MEASUREMENTS  
ON THE AYLESBURY LOW-RISE HOUSING ESTATE

Part III

Additional Experiments

M. E. Greenway and C. J. Wood

**ENGINEERING LABORATORY**

**PARKS ROAD**

**OXFORD**

WIND TUNNEL PRESSURE MEASUREMENTS  
ON THE AYLESBURY LOW-RISE HOUSING ESTATE

Part III

Additional Experiments

M. E. Greenway and C. J. Wood

## 1. INTRODUCTION

The experiments described in this final part of the Aylesbury study are not concerned with the acquisition of further data. They represent simply an opportunity taken in passing, to take a brief look at some of the fundamental considerations concerning the nature and validity of the measurements themselves.

The first two chapters relate to the measurement of extreme pressures. In making these measurements, two time parameters must be decided. The first is the observation time, or the duration of the experiment, while the second is the averaging time. The latter specifies the upper frequency limit of the signal which is to be accepted. Both these parameters affect the numerical values of the extreme pressure data which is produced.

In the main experiment described in Part II, the choice of these times is constrained by the need to match, in dimensionless terms, the choices already made by Eaton and Mayne (1974) in connection with the B.R.E. full-scale experiment. Discarding this constraint, the following paragraphs describe some extra experiments designed to assess the effect of varying the observation and averaging times.

The final chapter describes an entirely different experiment. It is a brief attempt to assess the importance of the accurate simulation of the wind structure by a systematic variation of the statistical parameters one at a time.

## 2. EFFECT OF AVERAGING TIME ON EXTREME VALUES

The authors are not aware of any general analysis of the effect of averaging time. However, a helpful qualitative indication may be gained by considering a particular case.

The analysis of Davenport (1964), also discussed by Greenway (1978) refers specifically to a Gaussian distribution. It yields convenient expressions for the reduced mode  $u_{\eta}(v,T)$  and dispersion  $b_{\eta}(v,T)$  of the associated extreme value probability function when the observation time is  $T$ . As in Part II, the 'reduced' parameters arise by considering a random variate  $\lambda(t)$  which has a mean value  $\mu$  and a variance  $\sigma_{\lambda}^2$ . In the classical universal formulation of the Gaussian distribution a reduced variate  $\eta(t)$  is defined by

$$\eta(t) = (\lambda(t) - \mu_{\lambda}) / \sigma_{\lambda} \quad (1)$$

When expressed in these terms, Davenport's expressions are

$$u_{\eta}(v,T) = \sqrt{2 \ln(vT)} \quad (2)$$

$$b_{\eta}(v,T) = 1 / \sqrt{2 \ln(vT)} \quad (3)$$

These expressions show the effect of averaging time through the parameter  $v$  which is the average zero-crossing frequency (one direction) of  $\eta(t)$ .

This may be expressed in terms of the second and zeroth moments of the power spectrum  $S_{\eta}(n)$ .

$$v^2 = \int_0^{\infty} n^2 S_{\eta}(n) dn / \int_0^{\infty} S_{\eta}(n) dn \quad (4)$$

Examining this equation, it may be seen immediately that if the spectrum  $S_{\eta}(n)$  is truncated by the application of a low-pass filter, or by the equivalent digital averaging operation (see Part II Appendix B) the effect will be to reduce the zero-crossing frequency. This decrease in  $v$  in turn reduces the mode value of the extreme probability function by equation (2).

In comparing this conclusion with the present pressure measurements, it must be acknowledged that the pressure signals, although random, are not

Gaussian. A second discrepancy is that the present experiments deal with extreme values of a variate obtained by regular sampling of the continuous pressure signal. This is in contrast with the Davenport analysis which is defined in terms of turning values (maxima or minima) of the analogue signal. Clearly these will always be more extreme than any single sample although in the limit, when the sampling frequency is very much higher than the Nyquist frequency, the results will be the same.

Despite these difficulties, it seems not unreasonable to extend the qualitative results of the Gaussian analysis to provide a theoretical indication that increasing the averaging time will reduce the magnitude of any measured extreme values.

In order to make an experimental examination of this effect, four representative pressure tappings are selected (5WW3, 3WE3, WR1E, ER1B) on the four major surfaces of the test house with the A32 wind direction. Extreme pressure modes  $u_L$  and  $u_H$  are extracted from Part II Appendix A for these holes with averaging times of 0.2, 2, 4 and 16 seconds (full scale equivalent). To produce the reduced modes in a form compatible with equations (1) and (2) values of the mean pressure coefficient (Part II Chapter 4) and of the RMS pressure coefficient, were also recorded. Because the RMS value is also a function of the averaging time, new values were measured for this experiment with low-pass filter settings calculated to correspond to each of the chosen averaging times by the equation (Greenway 1978).

$$n_{\text{cut-off}} = 0.44/T_{\text{av}} \quad (5)$$

The reduced modes  $u'_L$  and  $u'_H$  for the lowest and highest extremes respectively were then calculated according to the equation (also used in Part II)

$$u' = (u - \mu)/\sigma \quad (6)$$

The values thus obtained are assembled in Table I. Also shown in this table are measured values of the zero crossing rate  $\nu$  and of the corresponding

Gaussian equivalent mode calculated from equation (1)

The zero-crossing rate was measured directly in these experiments, rather than by integrating the power-spectrum. A specially designed signal conditioning unit was used, which incorporated a Schmitt trigger circuit to detect either upward or downward zero-crossings after the mean had been removed by a high pass filter. Pulses from the Schmitt trigger were counted in the computer over a suitable time interval in order to determine a value for  $\nu$ .

Table 1 shows that these zero-crossing rates and the corresponding theoretical mode estimates (equation 2) do not vary greatly over the four selected pressure tappings. They simply display the expected tendency to increase as the averaging time is shortened.

The measured extreme values also display this trend quite distinctly, but in a far less orderly manner. Because the Gaussian probability distribution is symmetrical, a single extreme value mode is sufficient to describe both the highest and lowest extremes. The pairs of experimental values however, are obviously not symmetrical but reveal a skewness in the distribution which is different for each of the four faces of the building.

An attempt is made in Figure 1 to correlate the experimental extreme values with the parameter  $\sqrt{2 \ln(\nu T)}$  suggested by the Gaussian theory. The number of pressure tappings is of course far too small to support a generalisation at this stage, but there is in Figure 1 some indication of two distinct correlations. The signs, which are irrelevant of course in the context of the symmetrical Gaussian distribution, have been omitted from the experimental values also for the purpose of this comparison, and it is seen that each pressure tapping yields one extreme value on one curve and the other on the alternative curve. The higher of the two curves departs significantly from the Gaussian prediction and also appears to contain the more relevant data, namely the highest extreme on the windward wall and the lowest extremes for the roof panels and the leeward wall.

TABLE 1

EFFECT OF AVERAGING TIME UPON EXTREME PRESSURES  
FOR FOUR SELECTED PRESSURE TAPPINGS  
(OBSERVATION TIME T = 1020 secs)

HOLE CODE	5WW3			5EW3			WR1E			ER1B		
MEAN $C_p \sim \mu$	0.527			-0.321			-0.672			-0.449		
AVERAGING TIME (SECS)	RMS	EXTREME		RMS	EXTREME		RMS	EXTREME		RMS	EXTREME	
	$C_p$	$C_p$		$C_p$	$C_p$		$C_p$	$C_p$		$C_p$	$C_p$	
	$\sigma$	$u_L$	$u_H$	$\sigma$	$u_L$	$u_H$	$\sigma$	$u_L$	$u_H$	$\sigma$	$u_L$	$u_H$
0.2	0.302	-0.294	2.444	0.143	-1.083	0.091	0.287	-2.614	0.584	0.191	-2.061	0.059
2	0.270	-0.106	1.708	0.135	-0.922	-0.005	0.232	-0.695	0.005	0.163	-1.180	-0.066
4	0.241	-0.040	1.476	0.120	-0.871	-0.045	0.205	-1.564	-0.132	0.143	-1.082	-0.143
16	0.159	+0.177	1.041	0.084	-0.611	-0.150	0.141	-1.125	-0.368	0.103	-0.847	-0.261

## REDUCED EXTREMES

	5WW3				5EW3				WR1E				ER1B			
	$u_L'$	$u_H'$	$v$	$u(vT)$	$u_L'$	$u_H'$	$v$	$u(vT)$	$u_L'$	$u_H'$	$v$	$u(vT)$	$u_L'$	$u_H'$	$v$	$u(vT)$
0.2	-2.72	6.35	7.788	4.24	-5.33	2.88	6.163	4.18	-6.77	4.38	12.979	4.36	-8.44	2.66	10.187	4.30
2	-2.34	4.37	2.158	3.92	-4.45	2.34	2.329	3.94	-4.41	2.92	2.329	3.94	-4.48	2.35	2.058	3.91
4	-2.35	3.94	1.306	3.79	-4.58	2.30	1.167	3.76	-4.35	2.63	1.708	3.86	-4.43	2.14	1.144	3.76
16	-2.20	3.23	0.418	3.48	-3.45	2.04	0.508	3.54	-3.21	2.16	0.578	3.57	-3.86	1.83	0.515	3.54

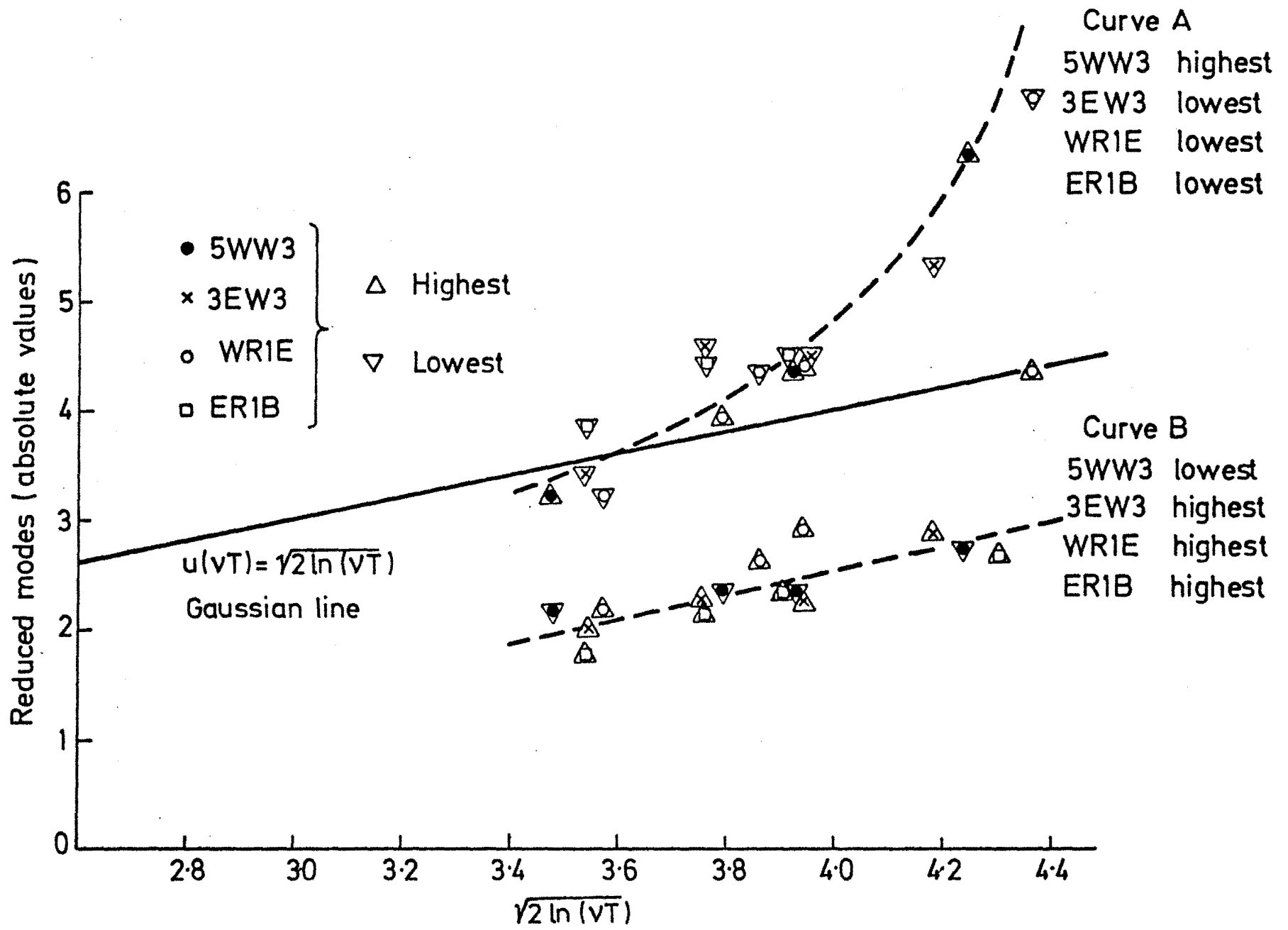


Figure 1

Effect of averaging time upon some measured extreme pressure coefficient modes



The form of the pressure coefficient probability distribution has been discussed by previous authors, e.g. Everett and Lawson (1977) who quote Peterka and Cermak (1975) and suggest that the distribution is Gaussian if the mean pressure coefficient is positive and that it has an exponential tail (beyond 3 standard deviations) when the mean pressure coefficient is less than  $-0.25$ .

The present results are not in conflict with the suggestion that a change in the character of the probability distribution occurs when the mean pressure is positive. However, the nature of that change seems here to be in the form of an inversion of the skewness rather than a change between two symmetrical distribution shapes.

Clearly there is room for further investigation of the best way to correlate this data.

### 3. EFFECT OF OBSERVATION TIME ON EXTREME VALUES

The Fisher-Tippett Type 1 extreme value probability distribution discussed in 1.3 describes the probability  $F_\lambda(n, r_\lambda)$  that in a single trial involving a random variate  $\lambda$  sampled  $n$  times (where  $n$  is large), the single extreme (largest of  $n$  or smallest of  $n$ ) sample will not surpass the value  $r_\lambda$ . The particular form of the Type 1 distribution is

$$F_\lambda(n, r_\lambda) = \exp\{-\exp[-(r_\lambda - u_\lambda)/b_\lambda]\} \quad (7)$$

This probability refers to a single future trial. If  $m$  whole future trials are considered, then the non-exceedence probability is reduced since it now becomes the probability that every one of  $m$  extreme values (or alternatively the extreme of  $mn$  samples) will not surpass  $r_\lambda$ . This probability is given by  $F_\lambda(mn, r_\lambda)$  where, if the trials are statistically independent

$$F_\lambda(mn, r_\lambda) = \{F_\lambda(n, r_\lambda)\}^m \quad (8)$$

Applying this prediction to the Fisher-Tippett type 1 distribution we may write

$$F_\lambda(mn, r_\lambda) = \exp\left\{-\exp\left[-\frac{r_\lambda - (u_\lambda + b_\lambda \ln(m))}{b_\lambda}\right]\right\} \quad (9)$$

Thus it is suggested that an increase in the observation period of an extreme value experiment will not change the dispersion  $b_\lambda$  of the resulting distribution but will merely increase the mode value from  $u_\lambda$  to  $u_\lambda + b_\lambda \ln(m)$ . The equation is valid for modes and dispersions either in dimensional or in reduced form.

In support of this general statement it may be observed that the Gaussian example, already used in the previous chapter, yields a similar result. When the observation period is extended from  $T$  to  $mT$  in equation (2), the mode changes to  $u_\eta(v, mT)$  where

$$\begin{aligned}
u_{\eta}(v, mT) &= \sqrt{2 \ln(vT)} \left\{ 1 + \frac{\ln(m)}{\ln(vT)} \right\}^{\frac{1}{2}} \\
&\approx \sqrt{2 \ln(vT)} \left\{ 1 + \frac{\ln(m)}{2 \ln(vT)} + \dots \right\} \\
&\approx u_{\eta}(v, T) + b_{\eta}(vT) \ln(m) \qquad m \ll vT \qquad (10)
\end{aligned}$$

Treating the dispersion in the same way, equation (3) may be used to obtain the approximation

$$b_{\eta}(v, mT) = b_{\eta}(v, T) - b_{\eta}^3(v, T) \ln(m)$$

which, when  $vT$  is large so that  $b_{\eta}(vT) \ll 1$ , reduces to

$$b_{\eta}(v, mT) \approx b_{\eta}(v, T) \qquad (11)$$

Set against this theoretical prediction it is of interest to examine some of the present experimental data for extreme pressure coefficients.

Using the same four holes previously selected on the test house, and repeating the A32 wind condition, the present extreme value experiments were repeated for observation times which were increased by factors of 2, 5 and 10, both for 0.2 second and 2 second averaging times. The results are recorded in table EXP 019 in Appendix A of Part II. Values from this table together with the basic results for the four holes in question from tables EXP 004, 010 and 012, are recorded in Table 2 below.

There is scatter but no observable trend in the dispersion results. Therefore for each case the average dispersion was used to produce values of the mode/dispersion ratio. These are then compared in Figure 2 with the theoretical prediction

$$\frac{u(m)}{b} = \frac{u(1)}{b} + \ln(m) \qquad (12)$$

The agreement found in these results is good and gives a measure of confidence in the present measurements of extreme values. It also confirms

that the equations

$$u(T_2) = u(T_1) + b \ln(T_2/T_1) \quad (13)$$

$$b(T_2) = b(T_1) = b \quad (14)$$

may be used with the present results to give a prediction of the extreme value probability function corresponding to an observation period other than the 17 minute period and for the present experiments.

TABLE 2

## EFFECT OF OBSERVATION TIME ON EXTREME MODES AND DISPERSIONS FOR FOUR SELECTED PRESSURE TAPPINGS

HOLE CODE	EXTREME HIGHER/LOWER	PARAMETER RECORDED	0.2 SEC. AVERAGES					2 SEC. AVERAGES				
			17 min	34 min	85 min	170 min	$\bar{b}$	17 min	34 min	85 min	170 min	$\bar{b}$
5WW3	HIGHER	u	2.444	2.543	2.940	2.928	0.255	1.708	1.803	1.953	2.270	0.160
		b	0.251	0.253	0.266	0.251		0.156	0.129	0.199	0.156	
		u/ $\bar{b}$	9.584	9.973	11.529	11.482		10.675	11.269	12.206	14.188	
	LOWER	u	-0.295	-0.328	-0.417	-0.470	-0.077	-0.106	-0.179	-0.224	-0.301	-0.066
		b	-0.085	-0.072	-0.063	-0.086		-0.075	-0.070	-0.052	-0.065	
		u/ $\bar{b}$	3.818	4.260	5.416	6.104		1.606	2.712	3.394	4.561	
3EW3	HIGHER	u	0.091	0.118	0.161	0.192	0.037	-0.005	0.043	0.060	0.105	0.031
		b	0.035	0.041	0.039	0.034		0.027	0.036	0.032	0.028	
		u/ $\bar{b}$	2.459	3.189	4.351	5.189		-0.161	1.387	1.935	3.387	
	LOWER	u	-1.083	-1.197	-1.334	-1.408	-0.159	-0.922	-0.981	-1.074	-1.202	-0.103
		b	-0.150	-0.176	-0.131	-0.178		-0.104	-0.089	-0.104	-0.115	
		u/ $\bar{b}$	6.811	7.528	8.390	8.855		8.951	9.524	10.427	11.670	
WR1E	HIGHER	u	0.584	0.717	0.982	1.018	0.197	0.005	0.139	0.261	0.381	0.121
		b	0.210	0.235	0.202	0.142		0.162	0.117	0.112	0.093	
		u/ $\bar{b}$	2.964	3.640	4.985	5.168		0.041	1.149	2.157	3.149	
	LOWER	u	-2.614	-2.613	-3.008	-3.168	-0.275	-1.695	-1.779	-1.832	-2.116	-0.167
		b	-0.293	-0.262	-0.278	-0.266		-0.176	-0.141	-0.189	-0.162	
		u/ $\bar{b}$	9.505	9.502	10.938	11.520		10.150	10.653	10.970	12.671	
ER1B	HIGHER	u	0.059	0.060	0.138	0.162	0.045	-0.066	-0.024	-0.003	0.162	0.031
		b	0.052	0.053	0.053	0.043		0.049	0.028	0.027	0.021	
		u/ $\bar{b}$	1.311	1.333	3.067	3.600		-2.129	-0.774	-0.097	0.419	
	LOWER	u	-2.061	-2.151	-2.658	-2.690	-0.310	-1.180	-1.203	-1.257	-1.489	-0.111
		b	-0.286	-0.280	-0.329	-0.346		-0.129	-0.103	-0.122	-0.090	
		u/ $\bar{b}$	6.648	6.939	8.574	8.677		10.631	10.838	11.324	13.414	

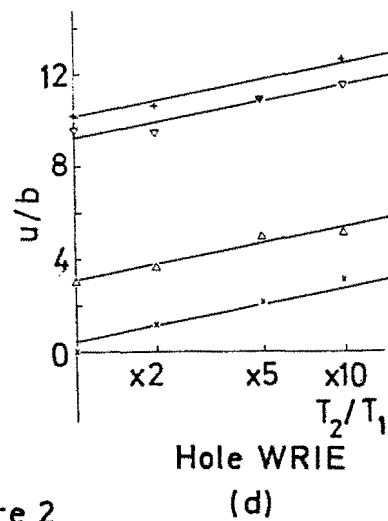
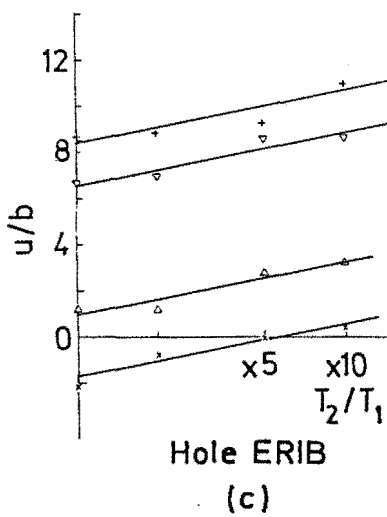
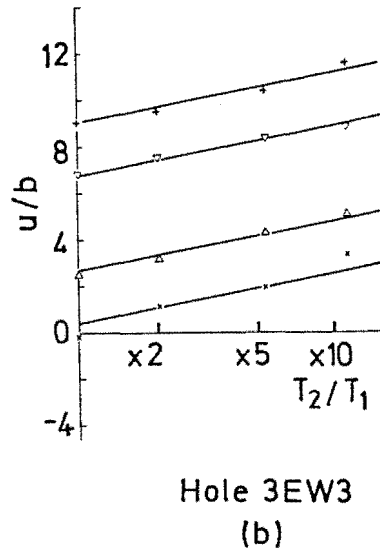
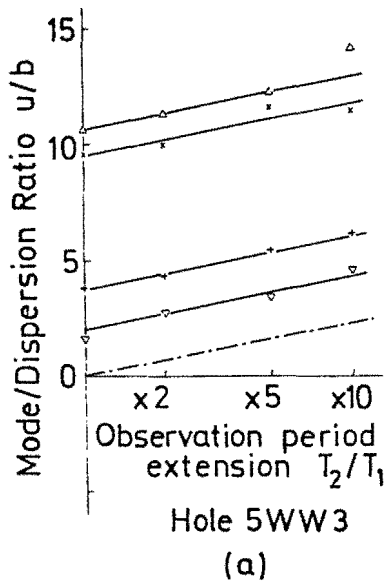


Figure 2

Effect of observation period upon some measured extreme pressure coefficient modes.

0.2 second averages x Highest extremes + Lowest extremes

2.0 " " Δ " " ∇ " "

APPLICATION

An immediate application of equations (13) and (14) arises in connection with one of the data comparisons of Part II Chapter 5. In discussing the comparison between the Oxford extreme pressure coefficient data and the corresponding data from the University of Western Ontario (Apperley et al. 1978) it was noted that the U.W.O. data was collected with an observation period equivalent to 150 minutes at full scale, whereas the Oxford experiments had been designed to correspond to the actual full-scale observation period of 17 minutes.

Because the U.W.O. results are in the form of single sample extremes, it is not possible of course to correct for this discrepancy. However for the purpose of achieving a time comparison it is possible to adjust the Oxford mode values to the U.W.O. observation period.

When applied to the reduced modes tabulated in Part II Chapter 4, equation (13) may be written

$$u'(150) = u'(17) + b' \ln(150/17) \quad (13a)$$

In order to display this calculation, extreme value data for Part II Chapter 4 is reproduced in Table 3 below. Linear regressions are then plotted in Figures 3 for the original data (see also Part II Figures 14a, b, c) and in Figure 4 for the adjusted data.

It was argued in Part II that although agreement cannot be expected between one single sample extreme value and any particular point in the extreme value probability distribution, a comparison involving many single point extremes is most logical if it is related to the mode of the distribution.

Applying this reasoning to the large number of one-to-one comparisons which make up a linear regression analysis, it is to be expected therefore that a regression slope of unity would indicate good agreement on average between the U.W.O. single samples and the Oxford Modes.

This comparison reveals the effect of the observation period adjustment in a most striking way. For the three unadjusted comparisons in















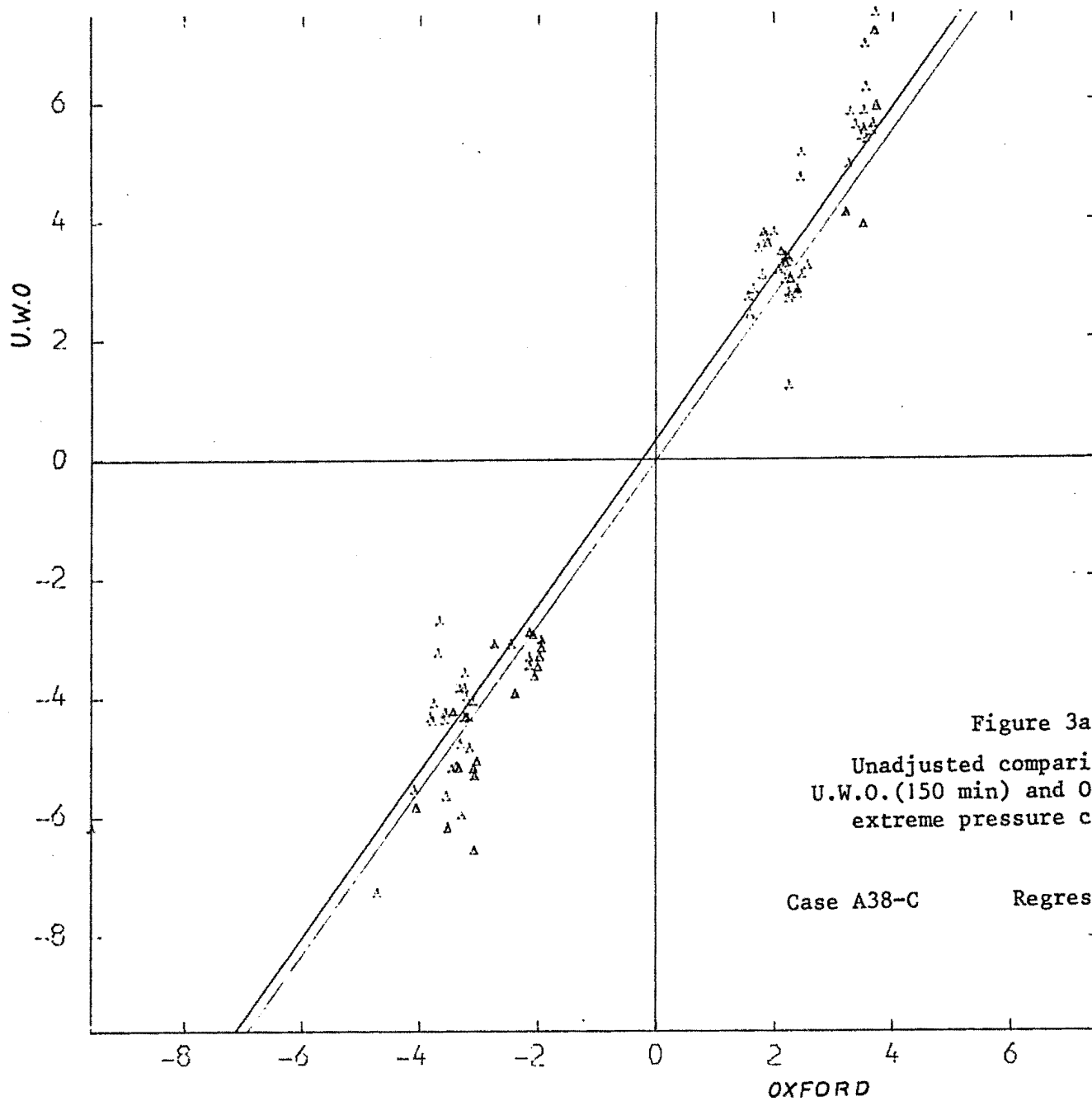


Figure 3a  
Unadjusted comparison between  
U.W.O.(150 min) and Oxford (17 min)  
extreme pressure coefficients

Case A38-C      Regression Slope 1.379

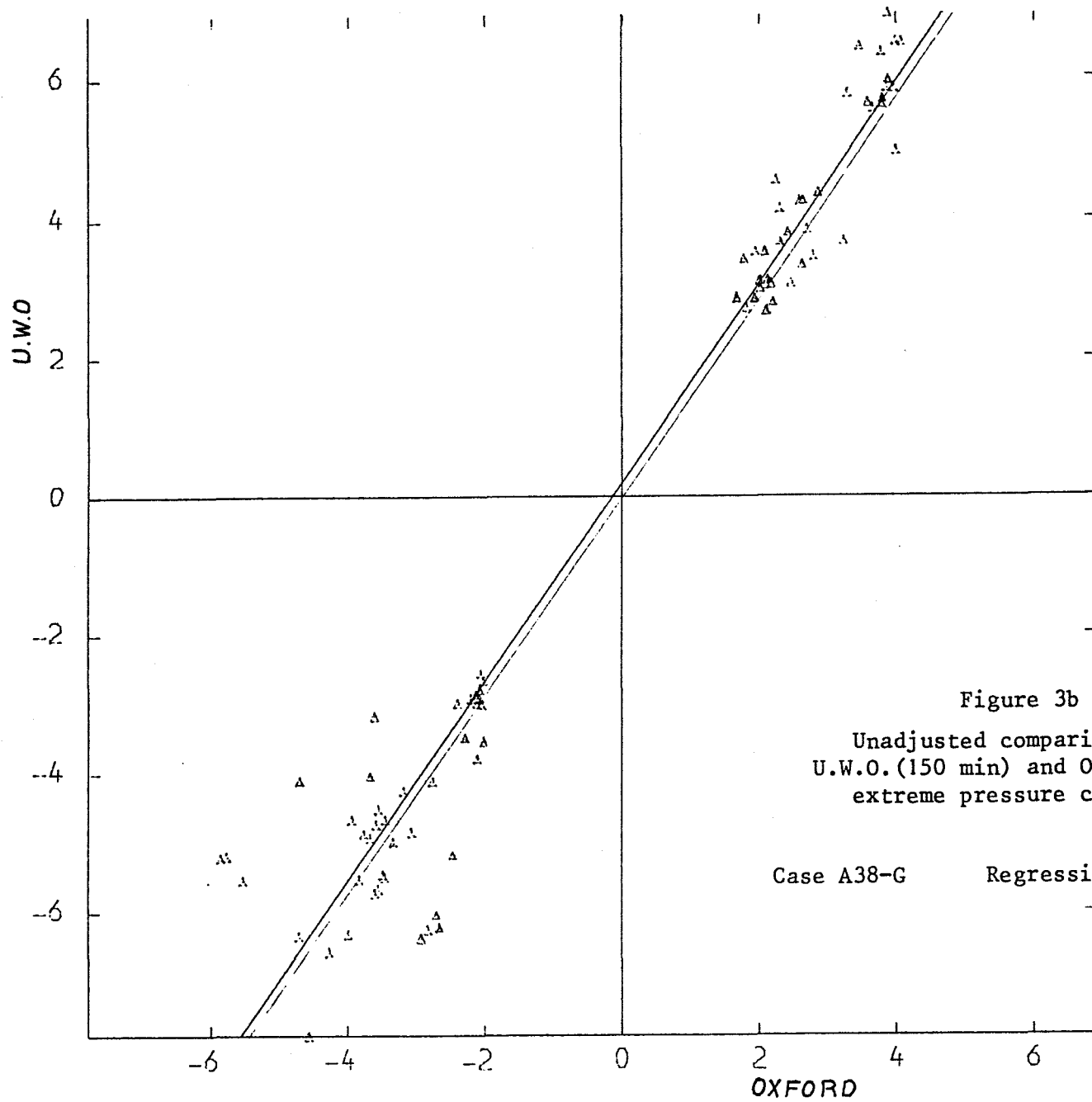


Figure 3b

Unadjusted comparison between  
U.W.O. (150 min) and Oxford (17 min)  
extreme pressure coefficients

Case A38-G

Regression Slope 1.430

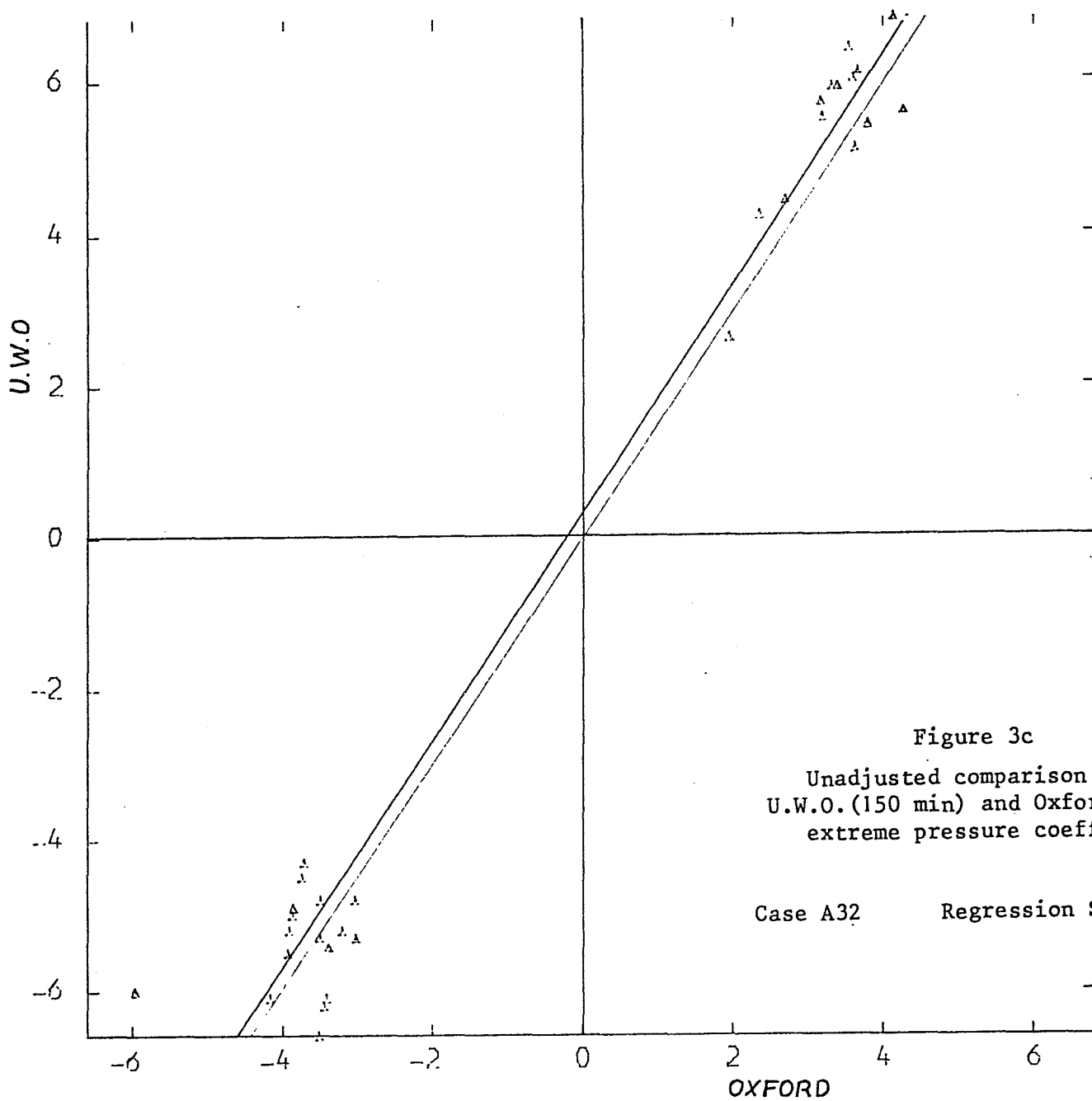


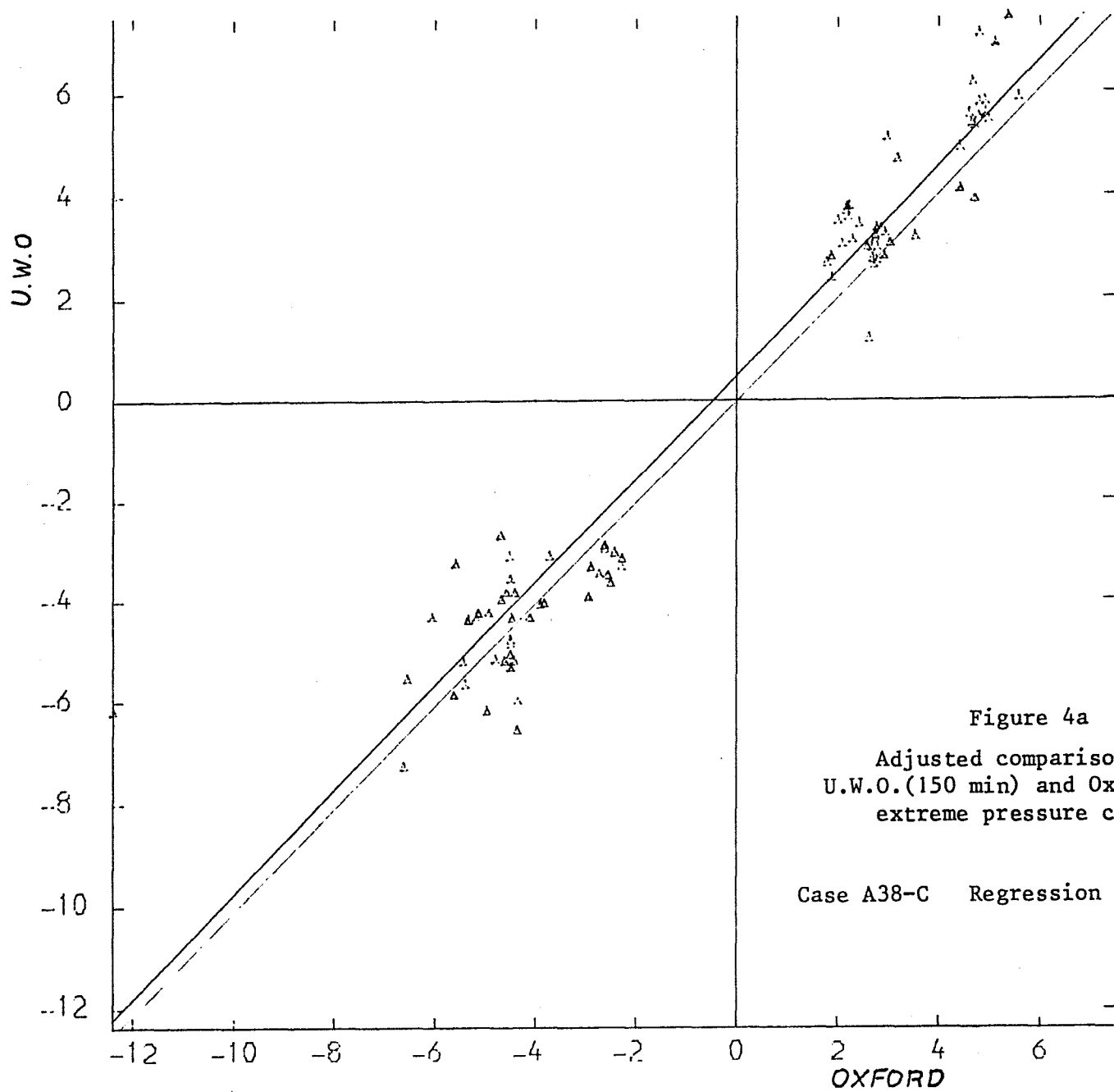
Figure 3c

Unadjusted comparison between  
U.W.O. (150 min) and Oxford (17 min)  
extreme pressure coefficients

Case A32

Regression Slope 1.488





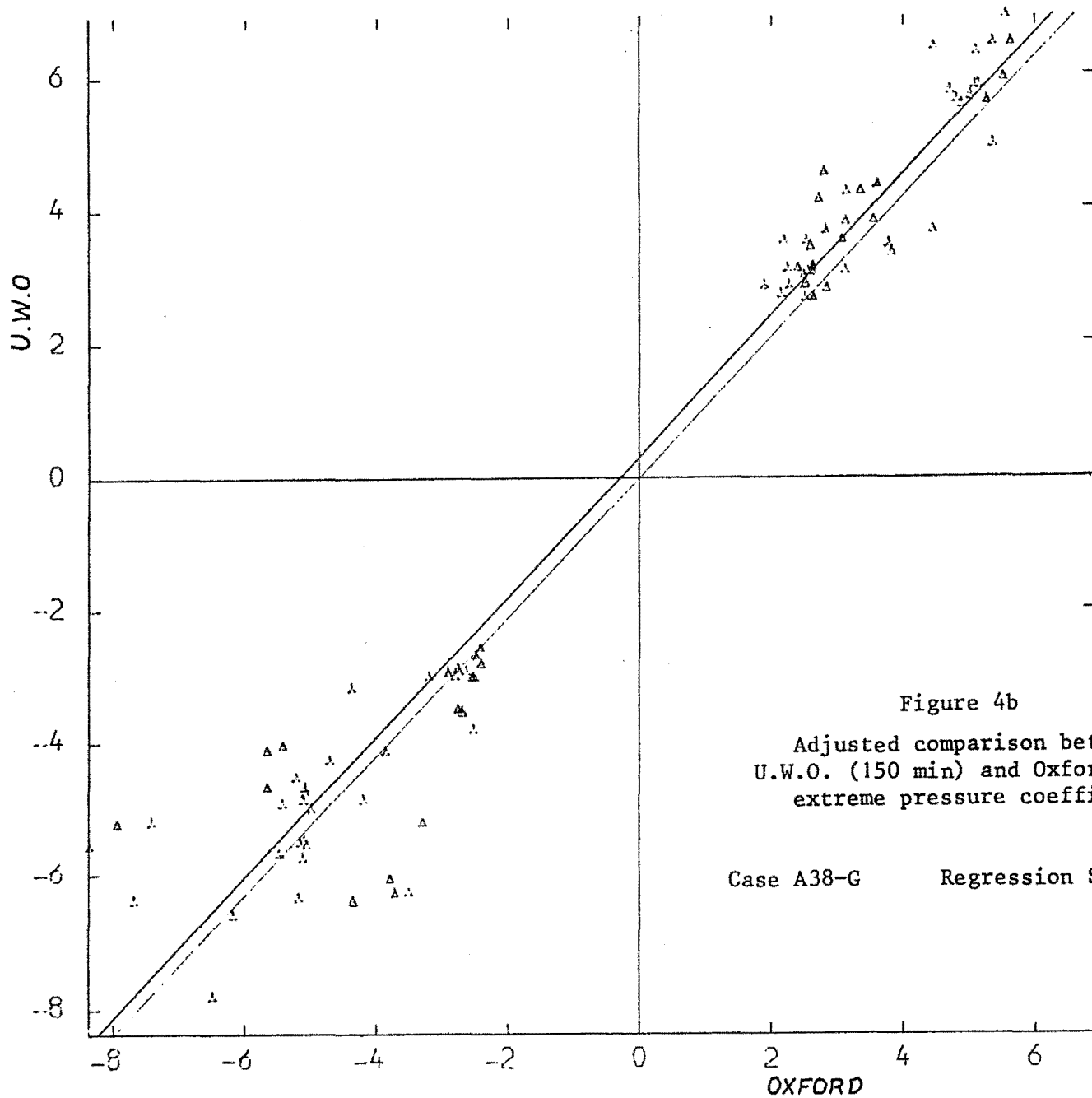


Figure 4b  
Adjusted comparison between  
U.W.O. (150 min) and Oxford (150 min)  
extreme pressure coefficients.

Case A38-G      Regression Slope 1.046

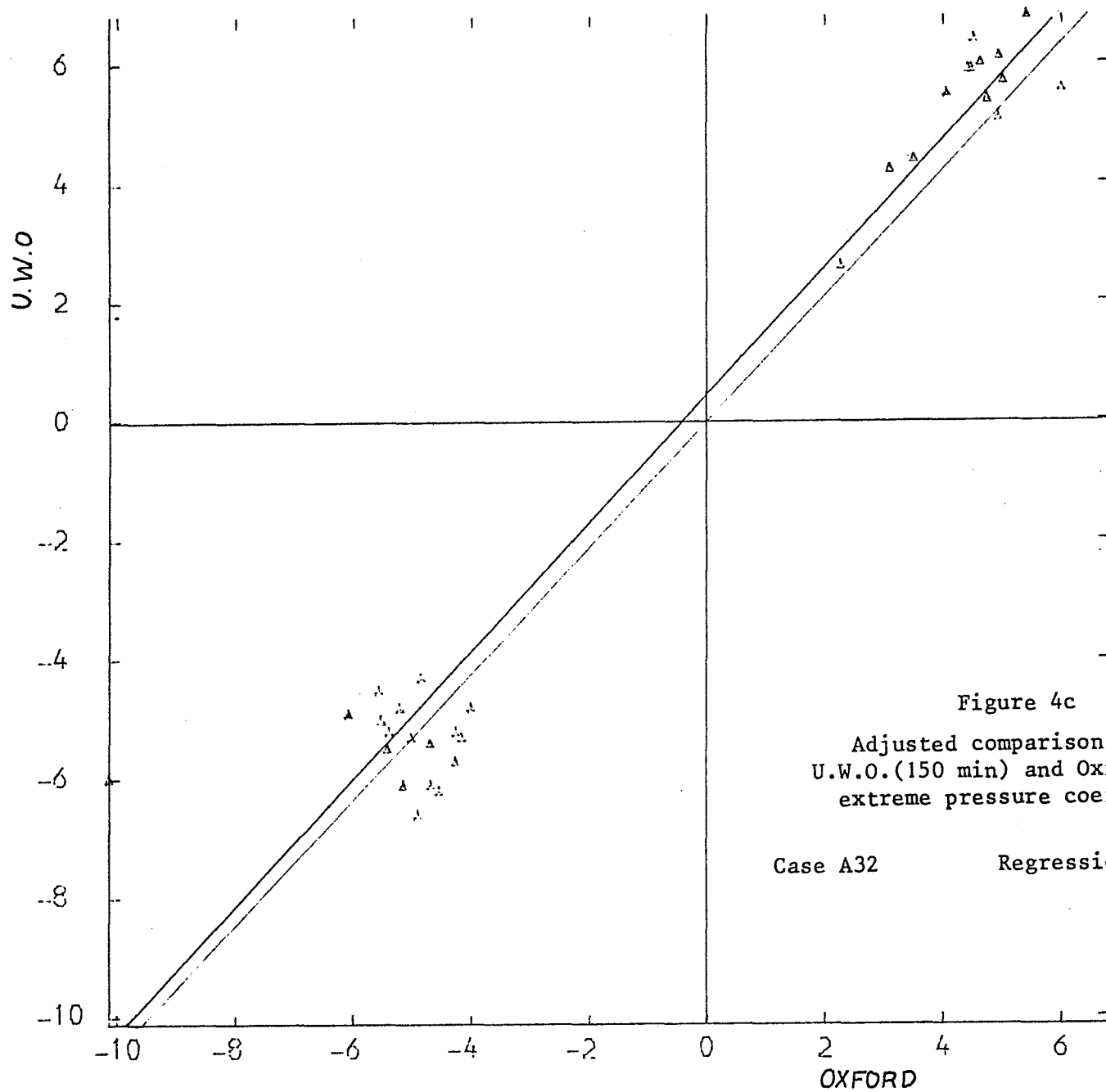


Figure 4c

Adjusted comparison between  
U.W.O.(150 min) and Oxford (150 min)  
extreme pressure coefficients.

Case A32

Regression Slope 1.056

Figure 3 the average regression slope is 1.43, indicating that the U.W.O. extremes are considerably higher than the Oxford values. After adjustment of the Oxford modes to the 150 minute observation time however, the agreement becomes very good indeed, with an average regression slope in Figure 4 of 1.04.

It is often argued that the present method of estimating extreme values, which involves at least sixteen repetitions of each data sampling experiment, is too costly in terms of tunnel time to be an acceptable technique. However, the success of the observation time adjustment procedure illustrated above suggests that the method need not be as time consuming as would appear at first sight. There is surely a case to be made for an investigation of an optimum procedure involving multiple repetitions, not of the full observation period but of a shorter period which can then be extended analytically by means of equations (13) and (14) to yield a prediction of the required extreme value mode and dispersion values.

A disadvantage of such a procedure is that it requires the use of the dispersion as well as the mode (Equation (13)). This introduces greater uncertainty because neither the Gumbel method nor the Lieblein method are capable of predicting dispersion values as accurately as they predict modes. For the 16 point scheme used here, it is shown by Greenway and Wood (1978) that while the standard error for the mode is only 3%, that for the dispersion is 21%.

#### 4. EFFECTS OF DISTORTED WIND SIMULATION

The dependence of wind tunnel measurements upon the correct simulation of the wind structure is acknowledged formally by the insertion of the generalized descriptor  $\phi(Z)$  in equation (1) of Part II. The strength of the dependence is now generally recognised, so that most investigators devote considerable effort to the development of a tunnel flow whose measurable statistical characteristics match as closely as possible the characteristics of the full scale wind over the given site, insofar as these are known.

Such is the importance attached to establishing the right simulation, and so tedious are the experimental adjustments required to approach it closely, that few investigators<sup>\*</sup>, having produced an acceptable flow, can summon the enthusiasm to experiment further to discover how their results would be affected if their simulations were not quite right.

The present authors experienced the same disinclination. Nevertheless a small amount of time was devoted to an attempt to produce, and assess the effect of, a systematic distortion of the wind flow described in Part I. The aim was to vary one only of the measured parameters, whilst retaining unchanged the values of the others. After some experimentation it was found that by varying the width of the lower bar of the turbulence grid, the turbulence intensity profile could be spoiled with very little change in the mean velocity profile or the power spectral density distribution of the longitudinal turbulence. Figure 5 shows the details of two distorted simulations, one having a turbulence intensity increased by 20-25 per cent and the other with similarly reduced turbulence. These are compared with the original simulation described in Part I.

Having achieved this distortion involving the turbulence intensity alone, pressures were re-measured at selected points on the model. Mean pressures showed no significant change but, as expected the RMS and extreme pressure coefficients (relative to the mean but not normalised with respect

---

\* An exception in this respect occurs in the work of Apperley et al. (1978) who show results for more than one simulation.

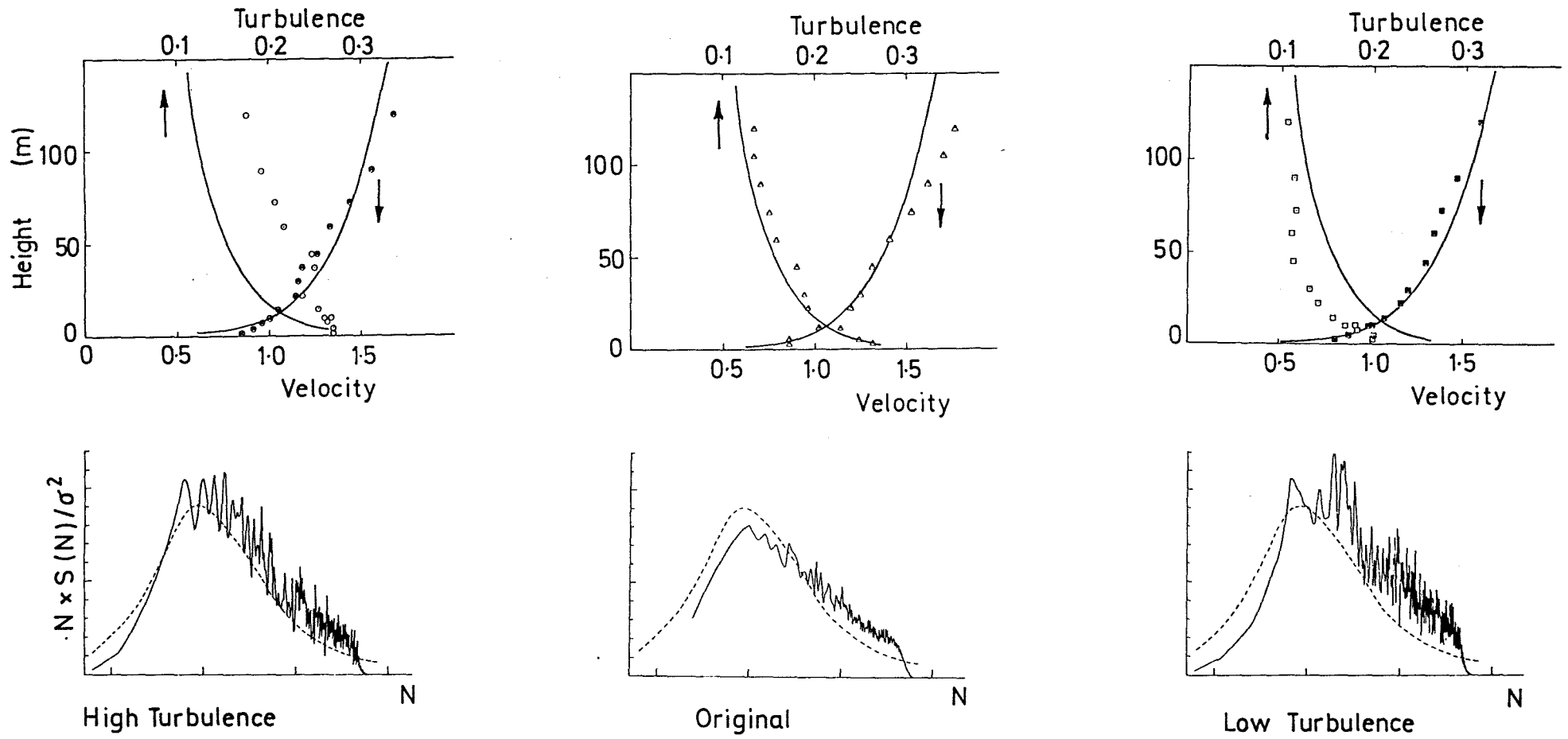


Figure 5

Comparison of distorted wind simulations

to the RMS) both showed a consistent increase with the turbulence intensity of the onset flow. This is illustrated in Figure 6 by the RMS pressure profiles for house 58 and also in Figure 7 by the well correlated linear regression comparisons for the test house.

Typically, the changes in RMS pressure appear to be similar in magnitude to the changes in onset turbulence intensity although there is no indication of a linear relationship. Indeed, it is to be expected that finite RMS pressures will occur even in a non-turbulent onset flow, since an architectural model produces its own turbulence.

The changes in the extreme pressures are less pronounced, suggesting that the fundamental shape of the probability distribution is not merely scaled but is also distorted by the changed onset turbulence.

Attempts to extend the experiment by producing isolated changes in either the spectrum or the mean velocity profile were not successful in the limited time allocated to this part of the programme.

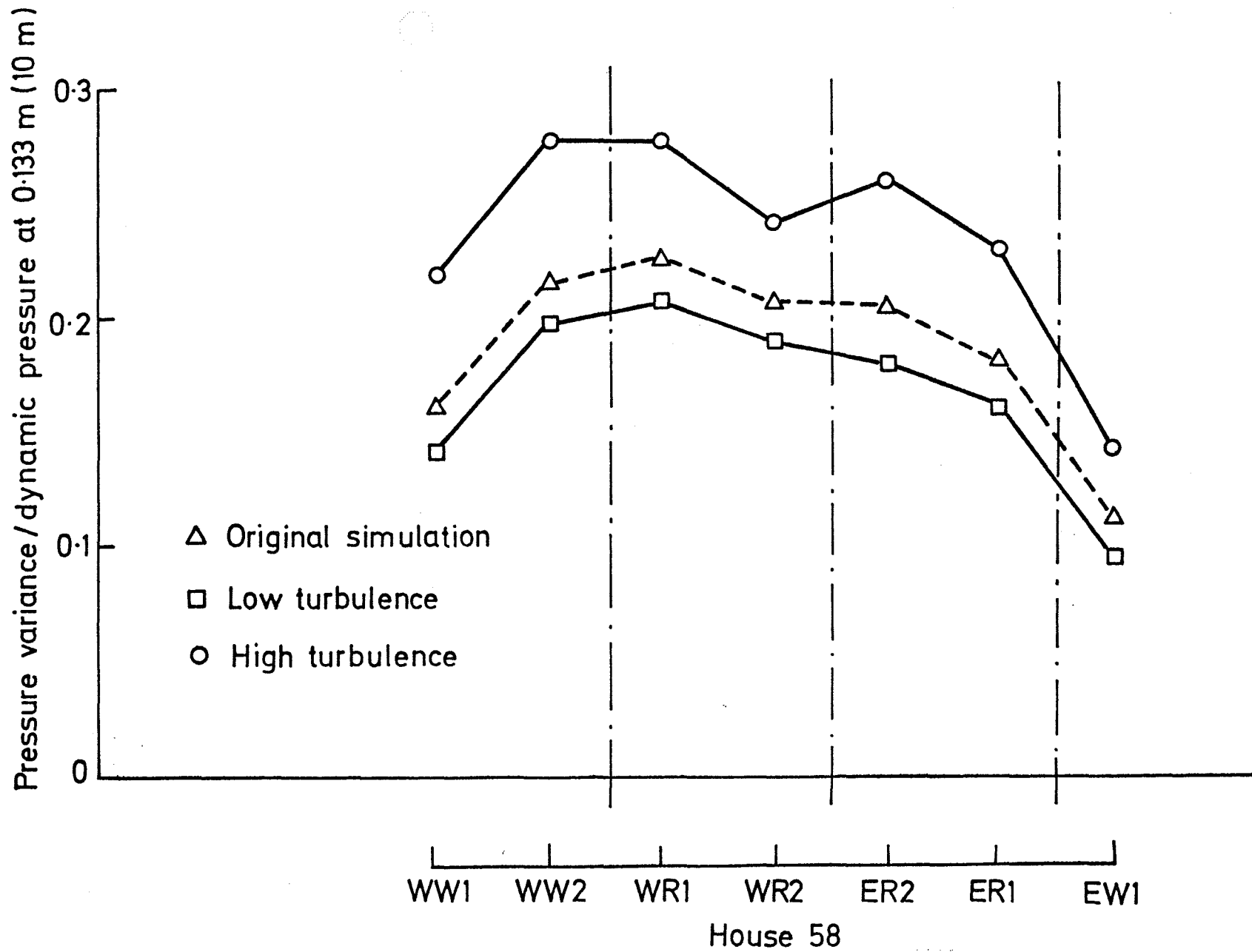


Figure 6

Effect of changed turbulence levels upon R.M.S. pressure coefficients (House 58)



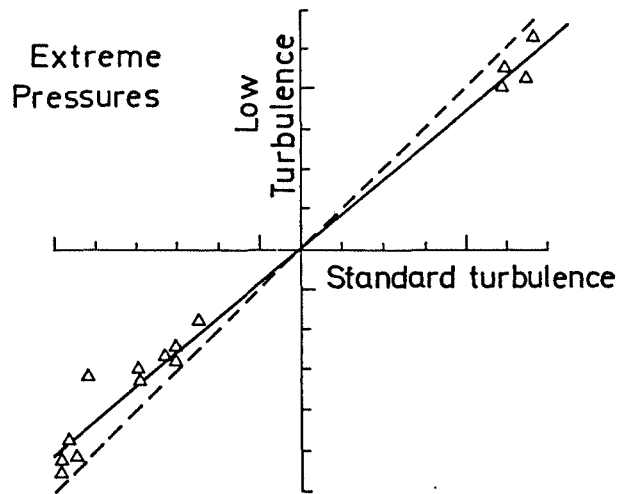
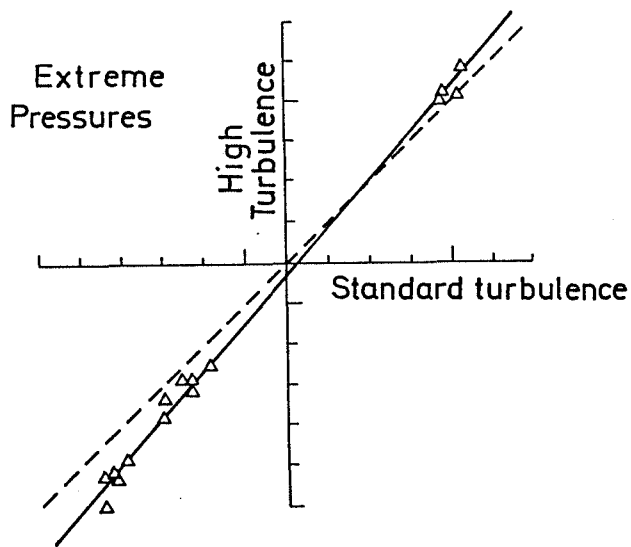
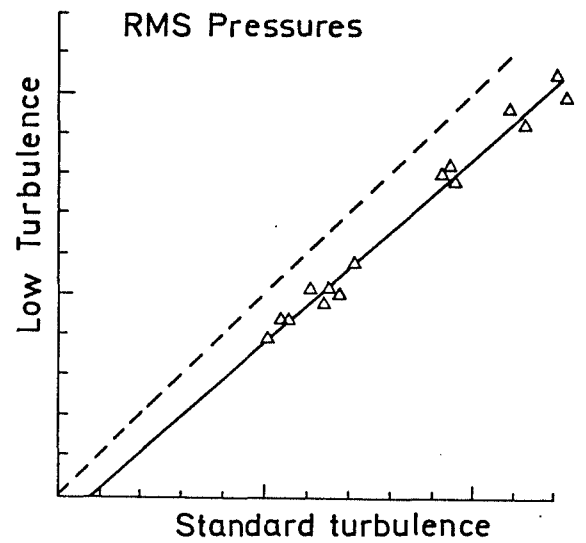
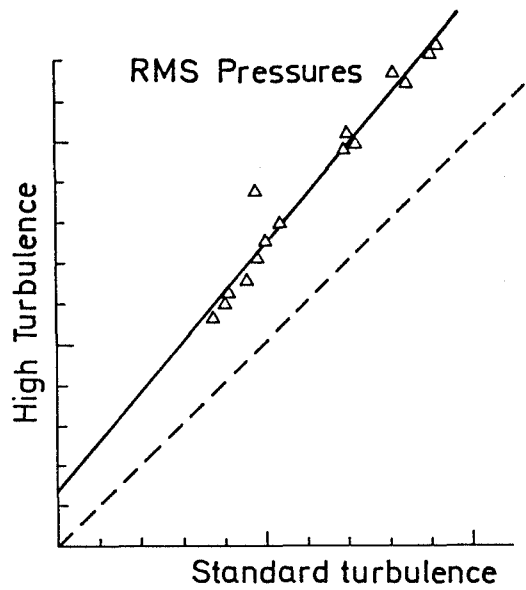


Figure 7.

Effect of changed turbulence levels upon R.M.S. and extreme pressure coefficients. (Test house)

